Nanometric ionic-liquid films on silica: a joint experimental and computational study

2009 J. Phys.: Condens. Matter 21 424118

(http://iopscience.iop.org/0953-8984/21/42/424118)

J. Phys.: Condens. Matter **21** (2009) 424118 (11pp) doi:10.1088/0953-8984/21/42/424118

Nanometric ionic-liquid films on silica: a joint experimental and computational study

S Bovio[1,2], A Podestà[1,2], P Milani[1,2], P Ballone[3] and M G Del Pópolo[3]

[1] C.I.Ma.I.Na, Università degli Studi di Milano, via Celoria 16, 20133, Milano, Italy
[2] Dipartimento di Fisica, Università degli Studi di Milano, via Celoria 16, 20133, Milano, Italy
[3] Atomistic Simulation Centre, Queen's University, Belfast, BT7 1NN Belfast, UK

E-mail: m.del-popolo@qub.ac.uk

Received 24 April 2009, in final form 27 June 2009
Published 29 September 2009
Online at stacks.iop.org/JPhysCM/21/424118

Abstract

Atomic force microscopy images for [bmim][Tf_2N] films deposited at ambient conditions by drop-casting show a population of terraced islands of mesoscopic area (1–100 μ^2) and ∼50 nm height. The regularity of terraces and steps, stiff mechanical properties and a fragile fracture mode all suggest that the islands are solid-like, even though bulk [bmim][Tf_2N] is liquid at the temperature of the experiment. Molecular dynamics simulations for a homogeneous [bmim][Tf_2N] film 4 nm thick on silica also display marked layering in proximity to silica of periodicity closely matching the experimental estimate of the step height. The density modulation of the simulated sample, however, decays into an approximatively homogeneous and fluid-like density distribution ∼2 nm from the solid surface. The detailed comparison of experiments and simulations is contained in the closing section of the paper.

(Some figures in this article are in colour only in the electronic version)

1. Introduction

A wide potential for applications coupled to favourable environmental properties have made room temperature ionic liquids (ILs) one of the most extensively investigated subjects in chemical physics of the last few years [1]. The viability and eventual impact of several among the proposed applications, including electrochemistry and heterogeneous catalysis, strictly depend on the properties of ILs at the interface with solid phases. Interfacial properties play an even larger role in applications such as lubrication [2], in which ILs are confined in a narrow space in between solid surfaces.

Despite these reasons for interest, the exploration of IL–solid interfaces is still in its infancy. To be sure, several experimental and computational studies of surface and interfacial properties of ILs have been published in recent years, and new contributions are appearing at an ever quickening rate [3]. Nevertheless, surfaces and interfaces are more diverse and more challenging than bulk systems, and the pace of progress is, by necessity, correspondingly slower. More importantly, the number of possible combinations arising from all different ILs, solid surfaces, and experimental conditions make the exploration of these systems a virtually open-ended task.

To enlarge our knowledge of interfacial properties of ILs, we undertook an extensive investigation of thin IL films deposited on solid surfaces, using a combination of experimental and computational methods. Preliminary results obtained by atomic force microscopy (AFM) on the morphology of 1-butyl-3-methylimidazolium bis-trifluoromethanesulfonylimide ([bmim][Tf_2N]) films deposited on the surface of silica, mica, and highly oriented pyrolytic graphite (HOPG) have been published recently in [4] and [5]. Here we focus on the case of [bmim][Tf_2N] on silica, and we discuss in detail the comparison of experimental data with the results of computer simulations carried out for the same system at comparable thermodynamic conditions.

In our experiments the solid substrate is represented by either an ordered silica surface, obtained by oxidizing a Si(110) layer, or by the surface of amorphous silica. At

the conditions of our experiments, both surfaces are expected to be largely hydroxylated, with comparable densities of OH groups. The ionic-liquid film is obtained by drop-casting, i.e. by first dissolving [bmim][Tf_2N] in methanol, and then spotting a few microlitres of solution onto the silica surface. Evaporation of the solvent leaves a thin IL deposit on the surface, whose structure, in principle, might depend on the deposition protocol. The chemical composition of the film, however, is free from appreciable contamination from the deposition solvent, as verified by x-ray photoelectron spectroscopy [4]. The resulting interface, analysed by AFM imaging, consists mainly of IL islands randomly distributed on the silica surface. Measurements of the surface topography emphasizes the regularity in the vertical organization of the islands, made of wide terraces and sharp steps, that persists throughout the entire thickness of the overlayer, in some cases exceeding 50 nm. The lateral size of the islands extends up to a few μm. In the case of amorphous silica, more rounded liquid droplets sometimes are seen to coexist with the thin, layered IL islands, uniformly spread on the islands themselves, or on the original silica surface [4, 5].

Simulations are carried out by molecular dynamics based on an atomistic force field model, and concern a fairly idealized interface made of a nanometric [bmim][Tf_2N] film ~4 nm thick, homogeneously spread over a fully hydroxylated β-cristobalite(111) surface.

Comparison of experimental and computational results reveals clear similarities between the two sets of data, as well as important differences. At all temperatures the simulation results display an apparent layering of the IL density in the direction z perpendicular to the surface. At room temperature the wide amplitude modulation of the IL density extends well into the liquid side of the interface, and is apparently reminiscent of the layering seen in the AFM images of thin IL islands. Moreover, the interlayer separation is very similar in the experimental ($\delta = 0.56$ nm) and in the simulated ($\delta = 0.60$ nm) samples.

Layering, however, appears to be far more marked in the experimental than in the simulation samples. The sequence of terraces and steps characterizing the shape of the islands seen in AFM images extends up to nearly 100 layers. Even at $T = 300$ K, four molecular layers at most are clearly defined in the IL density profile computed by simulation, and density appears to be nearly uniform beyond ~2.5 nm from the interface.

Moreover, the strict regularity of the step height, and the remarkable time stability of the structures seen by AFM, extending up to several months, suggest that [bmim][Tf_2N] islands on silica are solid-like, and perhaps crystalline, at ambient conditions. This conclusion is supported by AFM measurements of mechanical properties, showing that the basic framework of IL islands is surprisingly stiff, and even displays a fragile character upon fragmentation. This observation is particularly remarkable, since bulk [bmim][Tf_2N] is fluid at the temperature of the experiment, and even for a molecular system such as [bmim][Tf_2N] the thickness of the layered islands is already well within the mesoscopic range. On the other hand, the simulated IL films appear to be liquid-like down to $T = 350$ K. Their thermodynamic state is less certain at $T = 300$ K, since relaxation mechanisms and dynamics are very slow on the simulation timescale, and the IL film shares properties of liquid and glassy systems. Nevertheless, the simulated system is apparently not solid-like, and much less crystalline.

A second remarkable feature revealed by simulation is represented by an apparent density peak in the uppermost portion of the IL layer. This density anomaly, already seen in previous simulations for the free surface of IL [6], has been confirmed by x-ray reflectivity measurements [7] and by sum frequency vibrational spectroscopy (SFVS) [8] for systems closely related to the one considered in the present simulations. This feature, however, is not apparent on the scale of our AFM measurements for the thin [bmim][Tf_2N] film on silica, showing that the height of all IL planes is virtually the same across the entire width of the layered islands.

The reasons underlying these apparent differences between computations and experiments are discussed in section 4 of our paper. Understanding and possibly extending the validity and reliability limits of the computational model is clearly a very important target for our study, since, once validated, simulations could provide a wealth of microscopic information on the structure and dynamics of the interface. Examples reported in section 3 include the computation of the diffusion coefficient for anion and cation, the determination of the electrostatic properties of the interfacial double layer, and the analysis of correlation functions and orientational ordering for all species of interest.

The results of our investigations largely agree with those of previous studies whenever a comparison is possible. Layering and solid-like ordering in [$C_n$mim][X] ([X]$^-$ = [PF_6]$^-$, [BF_4]$^-$, [$PdCl_4$]$^-$) thin films on Si(111) covered with native oxide have been inferred from x-ray reflectivity measurements reported in [9]. In recent years, SFVS has been the method of choice to characterize the interface between ILs and solid phases. SFVS measurements on [bmim][Tf_2N] on silica and on closely related systems have been reported in the literature (see, for instance [10, 11]), documenting, in most cases, an apparent layered structure at the interface. Layering of the IL density has also been observed in [bmpy][FAP] on sapphire(0001) [12]. The fit of the experimental data with relatively simple models, however, suggests that in these cases the density modulation induced by the interface does not extend more than a few layers away from the solid surface. The difference from the experimental results reported here and from those of [9] might be due to the macroscopic width of the IL side of the interface, in contrast with the thin film configuration considered here and in [9].

Computer simulations for [bmim][Tf_2N] on ordered quartz surfaces have been reported recently in [13]. The simulation conditions and the results are closely related to our own computations. The simulations of [13], however, are meant to model an extended IL phase in contact with the solid surface. The thin IL slab, therefore, is enclosed in between two equivalent and parallel hydroxylated quartz surfaces, while in our computation we consider a thin film, deposited on silica and exposing a free surface towards vacuum. The

influence of the thin film geometry on the IL properties is in fact an important issue for our study. Moreover, the simulations of [13] are limited to fairly high temperature ($T \geqslant 400$ K). The results of our study, however, show that the most dramatic manifestations of layering take place at around room temperature.

Large amplitude layering of the IL density was also predicted on the basis of molecular dynamics simulations for [bmim][NO_3] on rutile (110) [14], and for [bmim][PF_6] on graphite [15]. The [bmim][NO_3] on rutile computations have close similarities with the simulations reported in the present paper. The computations of [15], although very interesting, rely on a model whose validity is somewhat more uncertain than in the oxide case, because of the semi-metal character of graphite, introducing, among other things, image charge interactions at the interface.

2. The experimental picture

2.1. Materials and methods

Two samples of the ionic liquid [bmim][Tf_2N] from Sigma Aldrich and from Queens University Ionic Liquids Laboratories (QUILL) were used, both with purity grade greater than 98.0%. Methanol, from Fluka, with 99.8% (HPLC) purity grade, was further distilled twice and used for preparation of solutions with the ionic liquid. Standard 13 mm diameter discs of amorphous silica (glass cover-slips) from Assing and squared, single-side polished specimens of Si(110) were used. Samples suitable for the investigation by AFM of the solid–liquid interface of [bmim][Tf_2N] have been obtained by drop-casting 20 μl of highly diluted solutions of [bmim][Tf_2N] in methanol (concentrations lower than $1 \times 10^{-2}/1 \times 10^{-3}$ mg ml^{-1}) on the substrates, allowing them to dry in ambient conditions. A comparative x-ray photoelectron spectroscopy analysis on a bulk of pure [bmim][Tf_2N] and on drops obtained by casting a concentrated methanol–IL solution confirmed that the solvent used in the deposition process does not react with the ionic liquid. All substrates were freshly prepared immediately before deposition of the [bmim][Tf_2N]–methanol solution. Amorphous silica and Si(110) substrates were cured in aqua regia solution (3 parts HCl–1 part HNO_3) before deposition in order to remove organics and re-hydroxylate their surfaces.

A Bioscope II AFM from Veeco Instruments was used. The AFM was typically operated in tapping mode in ambient conditions with standard single-crystal silicon cantilevers (resonance frequency between 200 and 300 kHz, nominal radius of curvature of the tip 5–10 nm). Typically, image scan size was between 5 μm $\times$ 5 μm and 20 μm $\times$ 20 μm, with scan rates in the range 0.5–1.5 Hz. Stable imaging conditions could be achieved and maintained for hours as if scanning on a solid surface. We did not observe significant changes in the imaging conditions when imaging in a dry nitrogen atmosphere. The AFM was also operated in force-spectroscopy mode, using force modulation tips with typical force constant $k = 4$ N m^{-1} and standard contact-mode tips with force constants in the range 0.06–0.6 N m^{-1}. When force spectroscopy is coupled to contact-mode imaging, several force-versus-distance curves are acquired along a raster pattern spanning a finite area, and built on a previously acquired AFM image. Each force curve is obtained recording the cantilever deflection (which is converted into a force, upon suitable calibration of the lever) as a function of the relative tip–surface distance [4].

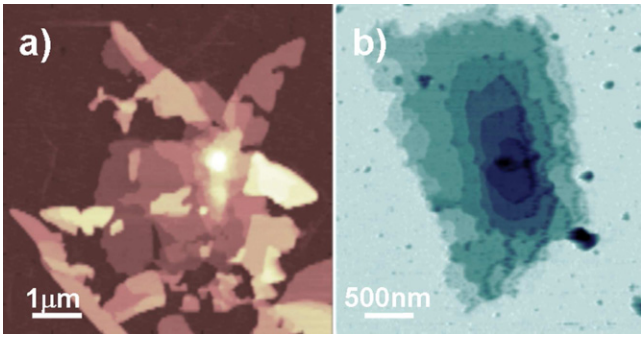

Figure 1. AFM topographic maps of thin [bmim][Tf_2N] films on (a) amorphous silica and (b) polished oxidized Si(110). The first map has been acquired in contact mode and the second one in tapping mode. Vertical colour scales 50 nm.

All depositions and measurements have been carried out in air at ambient conditions, i.e. at a nominal temperature of $T = 298$ K.

2.2. Statistical analysis of the heights of solid-like layers

Wide area scans of the silica surfaces following deposition show a population of randomly distributed and partly overlapping islands of ~1–10 μm lateral size (see figure 1(a)). Detailed topographic measurements on single islands (see figure 1(b)) reveal a layered structure, with wide flat terraces and sharp steps, extending throughout the entire island thickness, sometimes exceeding 50 nm. As discussed in detail below, islands appear solid-like under AFM measurements of their mechanical properties.

In a previous paper [4] we analysed the height of these solid-like layers by means of histograms of the heights calculated from the AFM topographies; this analysis has been performed to understand if the observed structures result from the regular vertical arrangement of a molecular layer with thickness δ. According to the schematic structural model shown in figure 2(a), we made the hypothesis that each terrace consists of several basic layers, and terraces with different heights are stacked one on top of the other. Figure 2(b) shows a typical height histogram of a layered structure. Such histograms consist of a series of peaks, each corresponding to a plateau in the AFM image. The peak-to-peak distances represent the average heights of piled-up terraces. Using an optimization procedure on terrace height data we find the best value of $\delta = 0.56 \pm 0.02$ nm for polished oxidized Si(110) and amorphous silica.

2.3. Test of the solid-like character of [bmim][Tf_2N] films

The force that the AFM probe exerts on the sample surface can be controlled. During imaging, the force is typically

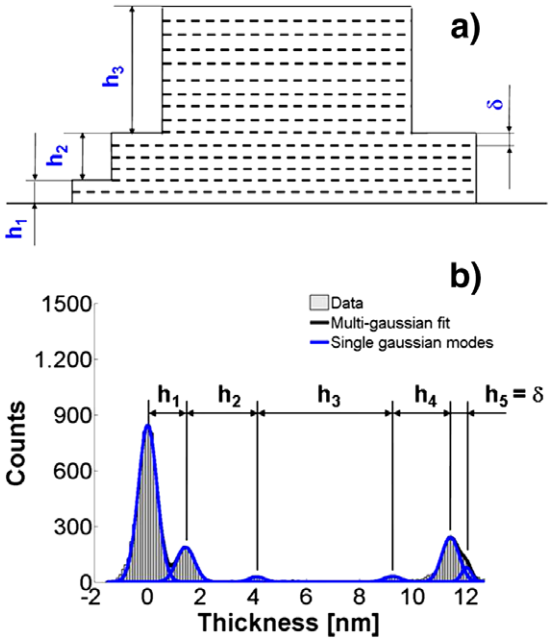

Figure 2. (a) Schematic representation of a layered structure. (b) Typical histogram of the heights of an AFM topography where terraces are present.

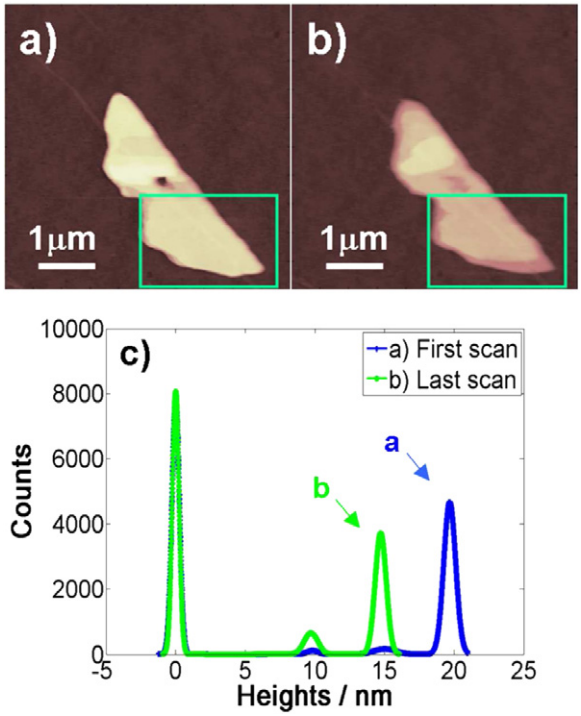

Figure 3. Delamination of [bmim][Tf_2N] layers on amorphous silica after three scans in contact mode. (a), (b) AFM topographies before and after delamination (vertical colour scales: 35 nm); (c) multi-Gaussian-fitted height histograms of the boxed regions in (a) and (b), showing that a top stack of basic layers disappears.

minimized, while in force-spectroscopy experiments it can be made large in order to test the mechanical resistance of the surface. We have collected evidence that the layered structures oppose a strong mechanical resistance to the AFM tip. We typically did not observe any scratch or penetration of the tip into the structures, even after repeated scans, and even when imaging in contact mode (in contact mode normal forces can be 10–100 times larger than in tapping mode, the contact pressure being of the order of 10–100 MPa). This proves that the layered structures are very compact, and in particular possess a strong mechanical resistance against vertical compression. The applied lateral force is expected to play a major role in disrupting the ordered [bmim][Tf_2N] films. Corresponding to the edges, the mechanical strength of the solid-like films is expected to be reduced, and therefore the lateral force exerted by the AFM tip can be enough to break the arrangement of the molecules. Noticeably, the applied lateral force is larger when the tip climbs the (steep) edges of the (higher) terraces, because the feedback loop of the AFM reacts with some delay to the quick changes of the topography. Stronger erosion is observed when imaging in contact mode because lateral forces are greatly increased with respect to tapping mode. Erosion observed in tapping mode is negligible. When imaging in contact mode at higher forces, delamination of a layered structure can also be observed. In figures 3(a) and (b) we show AFM images of the same terrace before and after repeated scans in contact mode at high force. It can be seen by comparing figures 3(a) and (b) that a complete stack of basic layers has been removed from the top of the terrace. Comparison of the height histograms before and after the scan (figure 3(c)) shows that the height of the removed layer is 10 times the height δ of the basic layer. This layer has been delaminated by high lateral forces during the first three scans. In fact, the strong peak at $h \sim 15$ nm grows at the expense of the peak at $h \sim 20$ nm, corresponding to the topmost terrace that has been swept away. AFM images and height analysis suggest that this structure behaves like a lamellar solid, which can be cleaved along preferential directions.

We have qualitatively tested the perpendicular hardness of [bmim][Tf_2N] layered structures by using the AFM in force-spectroscopy mode. We have acquired a topographic map of a terrace on polished oxidized Si(110) (figure 4(a)) and collected several force–distance curves along a grid, on the substrate as well as on the film. Figure 4(b) shows two approaching force curves, acquired on the silica substrate and on the film. The slopes of these curves in the contact region are the same. This suggests that the film behaves upon loading exactly as the hard silica substrate, which is like an impenetrable, solid surface. If deformation of the [bmim][Tf_2N] film occurred during contact, different slopes would be observed, together with discontinuities and irregularities in the first part of the linear region, witnessing the penetration of the film. We could not exclude however the possibility that a sudden and traceless penetration of [bmim][Tf_2N] film occurs immediately after contact. In this case the silica substrate, and not the film, would be loaded, and the slopes in the two force curves would be the same. We could rule out the occurrence of this event by observing that the two curves are horizontally shifted by an amount Δh corresponding to the thickness of the film (minus a height difference due to the presence of a clockwise tilt of the sample). In the case of penetration, this offset would be exactly equal to the height difference due to the tilt, and this

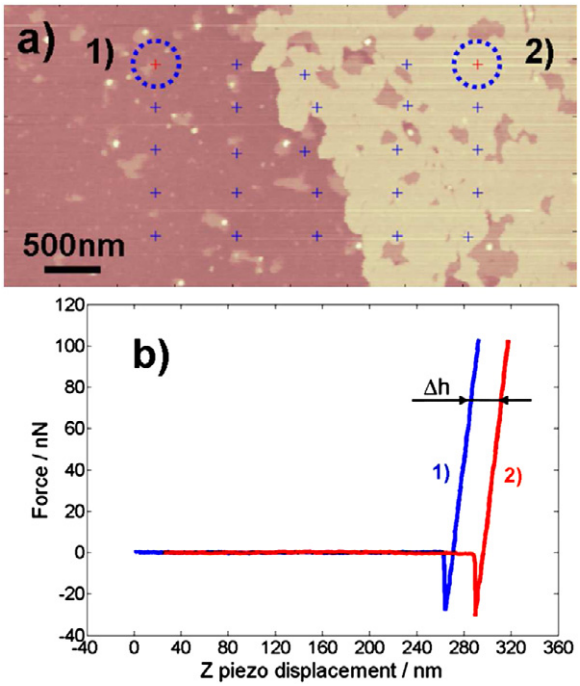

Figure 4. Test of the normal hardness of solid-like [bmim][Tf_2] layers on oxidized Si(110). (a) AFM contact-mode topography. A force–distance curve has been acquired in each point marked by a cross. (Vertical colour scale: 15 nm.) (b) Two representative force curves acquired in the circled locations, on the bare substrate (1), and on top of the IL layer (2).

is not the case. Same slopes and displacements are observed when much higher normal pressures (up to 1 GPa) are applied to the [bmim][Tf_2N] film (data not shown). These topography-related local force measurements provided a direct proof that the [bmim][Tf_2N] layered structures are solid-like.

3. Computer simulations

3.1. Model and simulation parameters

Computer simulations for an idealized but still realistic model of the experimental system have been carried out by molecular dynamics based on an atomistic force field, expressing the potential energy of the system as the sum of intra- and intermolecular terms. Intramolecular contributions account for bond stretching, bending and torsion, while intermolecular terms include dispersion and Coulomb interactions. The parameters proposed in [17] have been used for [bmim][Tf_2N], while the solid side of the interface is modelled using the potential of [18]. Intermolecular cross interactions are accounted for by combining the parameters of the IL and of silica using Berthelot's rule. All simulations are performed using the DL-POLY package [19].

A minimal representation of the solid side of the interface has been adopted for reasons of computational expediency. More precisely, the silica surface is represented by an oxygen and a silicon plane only, whose atoms reproduce the geometry of the Si terminated (111) surface of the β-cristobalite polymorph. Moreover, each Si ion in the terminal plane is decorated with one OH group, leading to an OH surface density of 4.1 OH groups nm^{-2}.[4] The stability of the solid surface is enforced by keeping fixed the positions of all the Si and O atoms in the simulated system, while the H atoms of the hydroxyl groups are mobile. This drastic simplification of the solid surface is justified by the fact that at room temperature the dynamics of the silica atoms is nearly completely frozen out because of strong covalent interactions and of quantum mechanical effects. Test computations for a single ion pair on a hydroxylated SiO_2 slab of increasing thickness have shown that atomic layers below the two top ones do not affect significantly either the adsorption energy and geometry, or the mobility of the ions on the surface. The simulated surface has a cross section of 54.9×52.8 $Å^2$.

The IL film is represented by 250 ion pairs, corresponding, at equilibrium, to a thickness of ∼4 nm. The orthorhombic simulation cell, of sides $54.9 \times 52.8 \times 170$ $Å^3$, is periodically replicated in 3D to mimic an extended system. The periodicity along z, in particular, is such that the IL film is separated by more than 130 Å from the closest repetition of the silica layer, thus ensuring a fair decoupling of replicated interfaces. Not surprisingly, given the relatively low temperature and the low vapour pressure of ILs, we never observe the evaporation of ions or ion pairs into the empty space in between periodic replicas. Coulomb interactions are dealt with using 3D Ewald sums. Constant temperature is enforced using a Nosé–Hoover thermostat.

3.2. Simulation results

A simulation sample consisting of 250 ion pairs in contact with an hydroxylated silica surface has been first prepared at $T = 600$ K, and then progressively annealed down to $T = 300$ K in steps of 50 K. At each temperature the system was equilibrated for 2 ns and we verified that no drift is apparent in running averages of computed properties after the equilibration stage. At $T = 300$ K, however, the system relaxation is very slow, and we cannot exclude the presence of a long term drift, undetectable by our statistical analysis. Production runs lasting 5 ns have been carried out at $T = 300$, 350 and 400 K.

The primary result of the simulation is the determination of the density profile for cations and anions along the direction z perpendicular to the interface. The ionic character of the system suggests to analyse the simulation trajectories representing each molecular ion by a single particle, carrying the full formal charge of the corresponding species. In what follows, the representing particle is located at the centre of the imidazolium ring for cations, while its centre coincides with the position of the N atom of the [Tf_2N] anion. Needless to say, this representation neglects the contribution of the butyl tails to the equilibrium structure of the IL film, that, however, will be discussed in more detail below. The total (anion + cation) density profiles for the representative ionic particles is shown in figure 5 for the three temperatures considered in our simulations.

[4] The experimental estimate of the OH density for fully hydroxylated amorphous silica surfaces is 4.9 ± 0.5 OH nm^{-2}, see [20].

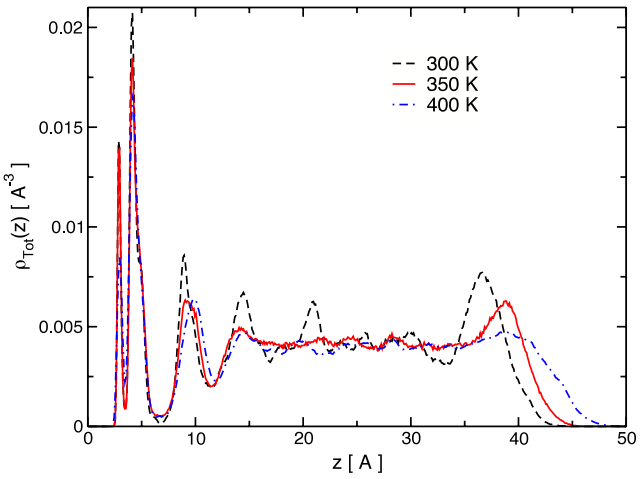

Figure 5. Total density profiles (cation plus anion centres) at 300, 350 and 400 K obtained from MD simulations of a [bmim][Tf_2N] film adsorbed on a hydroxylated SiO_2 surface. The surface area of the substrate is 2898.72 $Å^2$ and the OH concentration is 0.041 $Å^{-2}$.

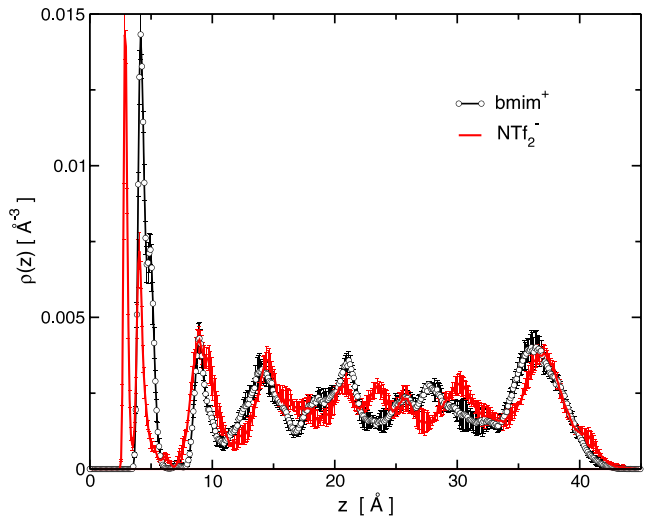

Figure 6. Cation (black with circles) and anion (red) density profiles at 300 K obtained from MD simulations of a [bmim][Tf_2N] film supported on hydroxylated SiO_2. Error bars calculated from five independent 1 ns trajectories.

First of all, the plot of figure 5 shows that the equilibrated IL film is ∼4 nm thick, and displays an apparent and sizeable thermal expansion with increasing T. In comparing our simulation results to the experimental data of section 2, it is important to consider that the simulated IL film is one order of magnitude thinner than the thickness of the solid-like islands imaged by AFM.

At all temperatures 300 K $\leqslant T \leqslant$ 400 K, the total density of ions displays a prominent double peak in close contact with the silica surface, followed by a regular succession of large amplitude density oscillations extending well into the IL film. Excluding the first two peaks, whose sharp profile is directly affected by the interaction with hydroxylated silica, the periodicity of the density oscillations turns out to be $\delta =$ 0.60 nm, independent of temperature to within the estimated error bar.

A second remarkable feature of the density profiles is apparent at the IL/vacuum interface, represented by a broad density maximum, overshooting the average density by more than a factor of two at $T = 300$ K.

As expected, the amplitude of the density oscillations induced by the silica surface increases with decreasing temperature. At $T = 300$ K, in particular, the wide density modulation of the first few IL layers is reminiscent of the apparent layering seen in the experimental images of terraced islands. Even at this temperature, however, oscillations do not extend more than 2.5 nm into the IL side of the simulated sample, whose central portion displays a nearly constant density, as expected in the case of fluid systems.

A slightly different picture, however, is suggested by the analysis of the total density in terms of cation and anion contributions, shown in figure 6 for $T = 300$ K. As apparent from this figure, the narrow region of nearly constant density at the centre of the slab results from the mutual cancellation of out-of-phase oscillations of the anion and cation densities, whose individual profiles display instead relatively sharp features, more characteristic of the glassy state than of a genuinely fluid system. The characterization of the system state as a glass is supported by the analysis of dynamical properties (see below). The distinction between a fluid and a glass, however, relies on the quantitative evaluation of properties such as the viscosity coefficient that are difficult to obtain by simulation, especially for an inhomogeneous system close to its melting point such as [bmim][Tf_2N] at $T = 300$ K. The precise identification of the thermodynamic state of the IL thin film, therefore, is rather uncertain at the lowest simulation temperature.

In parallel with the trend shown by layering at the silica–IL interface, also the height of the density anomaly at the IL–vacuum interface increases rapidly with decreasing T, while its width shrinks slightly. By contrast, the position and the shape of the double peak directly in contact with silica does not change appreciably over the 300 K $\leqslant T \leqslant$ 400 K temperature range.

Analysis of simulation snapshots, and of the density profiles for anions and cations, reveals that the sharp feature closest to silica in the prominent density doublet seen at low z in figure 5 is due to the $[Tf_2N]^-$ anion, whose oxygen atom accepts an H-bond from the OH groups at the silica surface. We estimated that, on average, only 60% of the OH groups available at the surface are engaged in a H-bond with $[Tf_2N]^-$, the saturation of the remaining hydroxyl groups apparently being prevented by steric constraints. The accumulation of surface charge due to the specific OH–anion bonding is compensated by the adsorption of a nearly equivalent number of positively charged imidazolium groups, giving rise to the second sharp peak in the doublet. As a result, and despite the fairly different interaction of anions and cations with the OH groups passivating the solid surface, the first IL layer in contact with silica turns out to be remarkably neutral.

The in-plane structure of the first layer in contact with silica has been visualized by identifying all ions whose distance from the reference surface plane is less than 4 Å.

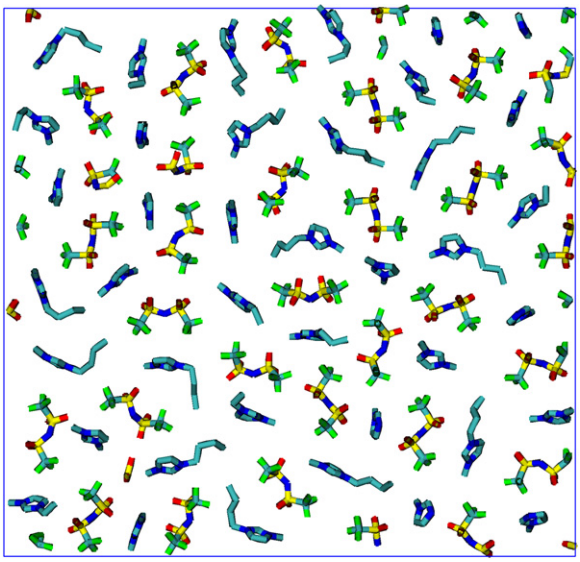

Figure 7. Snapshot of the first IL layer in contact with silica. Only ions separated by less that 4 Å from the silica surface are represented.

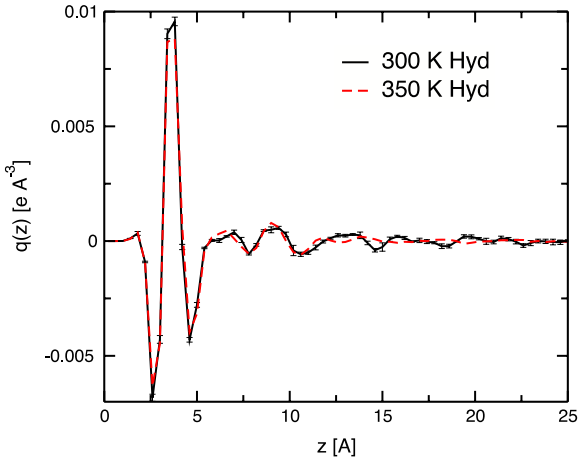

Figure 8. Charge density profiles, $q(z)$, calculated at 300 and 350 K.

Simulation snapshots (see figure 7 for the $T = 300$ K sample) highlight three major features: (i) a clear tendency to charge alternation, driven by strong Coulomb forces, responsible also for the near electrostatic neutrality of the first IL layer; (ii) apparent geometric regularities, hinting at crystal-like ordering for the in-plane distribution of ions, only marginally concealed by a sizeable concentration of defects; (iii) the depletion of the inner layer of cation tails. The distribution of ions on the surface appears to be in registry with the underlying surface lattice, even though the periodicity of the solid and IL layers appears to be different. Therefore, the in-plane regularity of the ion positions is likely to result mainly from specific interactions with the OH groups at the surface, introducing a sizeable corrugation of the xy potential felt by the ions. It is tempting to classify the motifs of positional disorder seen in figure 7 into localized (mainly substitutional) and extended (dislocation) surface defects, but the relatively small size of the 2D sample prevents an unambiguous identification. The study of crystal-like ordering, of defects, and, even more, of long-range interfacial correlations in the IL structure is an important and fascinating subject, whose investigation, however, requires coarse grained models and sophisticated statistical mechanics methods. The imidazolium rings in close proximity of silica tend to be oriented perpendicular to the surface, in qualitative agreement with the structural data extracted in [10] from sum frequency vibrational spectroscopy. Finally, the butyl tail depletion of the inner plane is apparently due to the preferential bonding of OH groups to the anion, and to the competing drive of the cations, due to local charge neutrality considerations. However, entropy might also play a role, since the solid silica surface limits the orientation and isomerization freedom of the hydrocarbon chain, effectively pushing it outwards.

The clear tendency of the IL to form neutral planes, already apparent from the structure of the first IL layer in contact with silica, is a dominant motif also for the few additional layers following the first one. The plot of figure 6 for the individual anion and cation probability distributions shows that, as expected, the two densities tend to vary in phase whenever the amplitude of the oscillation is sizeable, turning to charge alternation far from the surface, where the amplitude of the oscillations is small. The effectiveness of short-range screening at the interface, however, is somewhat remarkable for ions whose structure is so apparently different from each other. The strict enforcement of local neutrality is reflected in the plot of the charge profile (ρ_Q) along z (see figure 8), showing that the charge density is fairly small nearly everywhere. The oscillating character of $\rho_Q(z)$, however, still points to strong electrostatic and steric interactions, in apparent contradiction with the basic assumptions and results of simple theoretical approaches such as Gouy–Chapmann.

The numerical solution of Poisson's equation for $\rho_Q(z)$ shows that the inside of the IL slab tends to be at higher electrostatic potential than either the surface or vacuum. The total electrostatic potential drop across the interface (i.e. from silica to vacuum) turns out to be $\phi = 0.12$ V at $T = 300$ K, $\phi = -0.24$ V at $T = 350$ K and at $T = 400$ K, corresponding to an average dipole $d_z = 0.32$ Debye nm^{-2} at $T = 300$ K, and $d_z = -0.64$ Debye nm^{-2} at $T = 350$ and 400 K. The temperature dependence of ϕ and d_z is easily interpreted in terms of the relative displacement with changing T of the centre of mass R_z^+ and R_z^- of the cation and anion density distributions, respectively. A marked temperature dependence of all these quantities could have been expected, given the sizeable thermal expansion shown by the anion and cation density distributions. Nevertheless, the sudden change of sign in between $T = 300$ and 350 K is an intriguing observation, that might point to an incipient phase transition, either solid–liquid or para- to ferroelectric, taking place at about room temperature. Phenomena of this kind have already been detected in experiments for the surface of organic systems ([21]). In comparing simulation and experimental data, however, it is necessary to consider that in reality silica surfaces tend to be slightly charged [10], while the hydroxylated silica slab included in our simulations is strictly neutral.

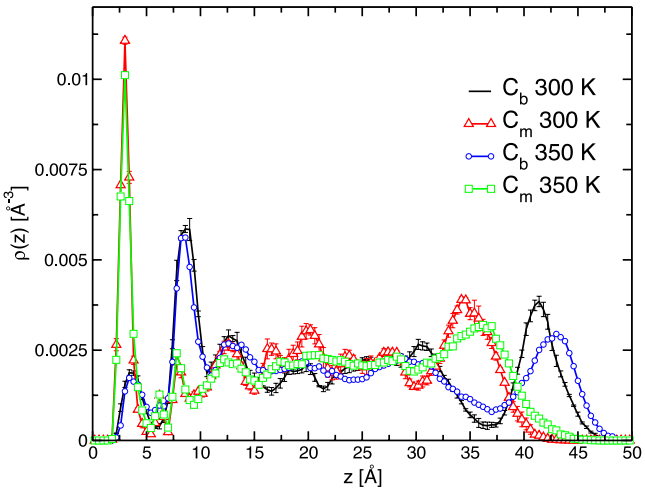

Figure 9. Density distribution of the methyl (C_m) and terminal butyl (C_b) carbon atoms of $[bmim]^+$.

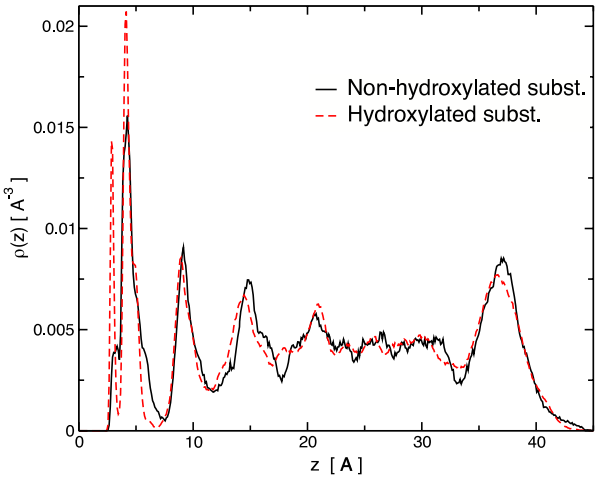

Figure 10. Density profiles for [bmim][Tf_2N] adsorbed on hydroxylated and non-hydroxylated SiO_2.

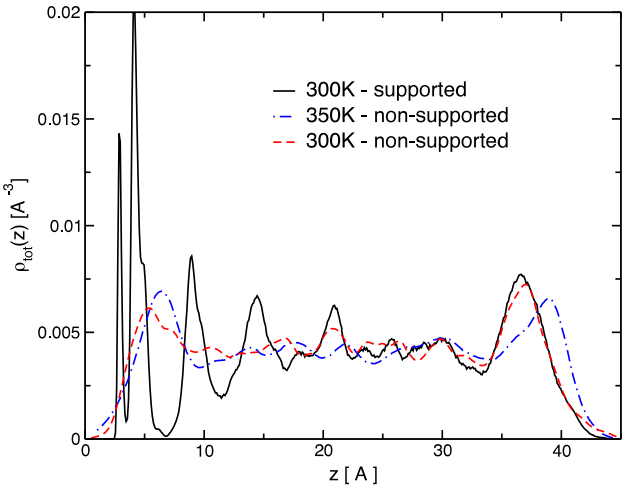

Figure 11. Total ionic densities for supported and non-supported films. Black continuous line: density profile for a [bmim][Tf_2N] film supported on hydroxylated silica at 300 K. Dashed coloured lines: density at 300 and 350 K for a free standing [bmim][Tf_2N] slab.

As already anticipated, the density profile at the IL–vacuum interface represents a second major feature of the simulated sample. As can be seen in figure 6, anions and cations contribute nearly equally to the broad density peak. Analysis of the spatial distribution of the butyl tails of $[bmim]^+$ show that they tend to segregate into a fairly thick external layer, extending up to 5 Å beyond the maximum of the ions density. The segregation of the hydrocarbon tails does not depend significantly on temperature, suggesting that potential energy and entropy both play a relevant role. These two thermodynamic potentials, in fact, might reinforce each other at the IL/vacuum surface. First of all, tails tend to stick out to enhance their rotational freedom, thus increasing their entropy. On the other hand, the depletion of tails in the immediate surface sub-layer allows a tighter packing of ions, giving rise to the density anomaly seen in figures 5 and 6, at the same time decreasing potential energy. The thickening of ILs at their surface predicted by simulations [6] has been confirmed by experiments [7, 8].

A more systematic view of the $[bmim]^+$ orientation relative to the surface is obtained by separately plotting the density distribution of the methyl (C_m) and outermost butyl (C_b) carbon atoms. The results shown in figure 9 for the $T = 300$ K simulated sample confirm the depletion of butyl tails in the first layer in contact with silica, and emphasize their enrichment on the vacuum side of the interface. The clear layering seen in between suggests that, at $T \sim 300$ K, the positional ordering already seen in the density profile is complemented by a sizeable degree of orientational ordering of cations (and presumably anions) throughout the entire interface. Once again, the simulation results agree at least qualitatively with the experimental data reported in [10].

The role of the OH groups in promoting layering at the solid-IL interface has been investigated by simulating the same IL slab in contact with a fully de-hydroxylated, oxygen terminated silica surface, meant to represent a prototypical hydrophobic surface. Starting from the thin silica slab used in the previous simulations, this second model of a neutral solid silica surface was obtained by replacing each terminal OH group with a single oxygen atom, whose charge is equal to the sum of the O and H charges in OH. As expected, the IL density peak closest to silica reduces upon this change, but the effect is quantitatively small (see figure 10), showing that IL layering is primarily due to the excluded volume effect represented by the solid surface [22], while the specific adsorption due to the OH–anion hydrogen bond mainly determine the height and detailed shape of the first peak.

On the other hand, removing completely the solid substrate restores both the symmetry of the slab and the fluid-like state of the IL (see figure 11). This observation is very important, because it confirms that the basic IL model is indeed liquid at $T = 300$ K (the experimental melting point of [bmim][Tf_2N] is $T_m = 267$ K, see [24, 25]) and, therefore, any glassy or even solid-like feature seen in the supported film must arise from the interaction between silica and the IL.

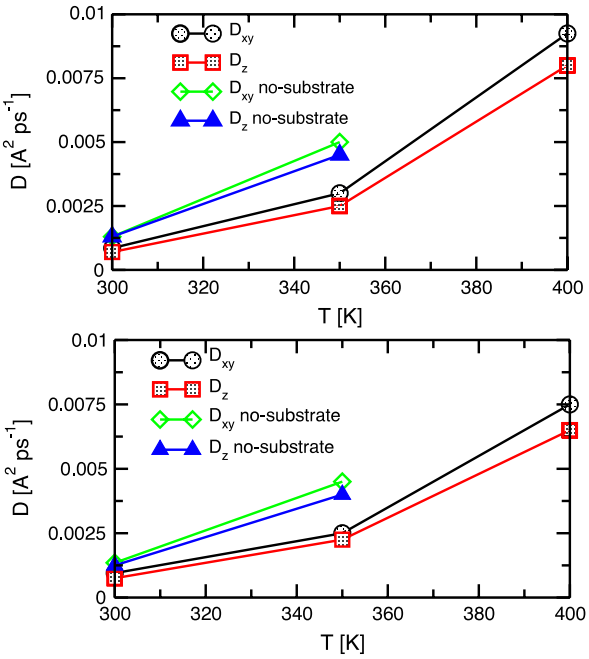

Figure 12. In-plane (D_{xy}) and out-of-plane (D_z) diffusion coefficients of cations (upper panel) and anions (lower panel) as a function of temperature for the solid-supported and the free standing [bmim][Tf_2N] slabs.

The in-plane (D_{xy}) and out-of-plane (D_z) diffusion constants[5] of cations and anions have been estimated from the asymptotic slope of the mean square displacement of ions as a function of time (i.e. using Einstein's relation). The temperature dependence of the anion and cation diffusion constants is displayed in figure 12). Diffusion is non-negligible down to $T = 350$ K, while at $T = 300$ K is at the limit of what we can estimate from simulations on the ∼5 ns timescale. Above $T = 300$ K, the diffusion constant of anions and cations is fairly similar, and, somewhat surprisingly, it is fairly isotropic. Moreover, removing the substrate enhances diffusion, supporting the conclusion that any glassy or solid-like feature shown by the system at $T = 300$ K is due to the interaction with the solid surface.

As a further characterization of the IL dynamics, we estimated the average time τ_R that ions in the inner region of the interface spend on each of the molecular layers identified by the density oscillations, before migrating to another one by thermal diffusion. The residence time of ions in the first layer in contact with silica turns out to be much longer than our simulations, and, therefore, it cannot be determined to any acceptable level of confidence. The residence times in neighbouring layers are also very long, in the several nanosecond range, and therefore they are also rather uncertain. By way of comparison, we computed the residence time τ_R of ions in a $\delta z = 4$ Å range located at the centre of the slab. The results, $\tau_R = 9$ ns at $T = 300$ K and $\tau_R = 3.2$ ns at $T = 350$ K are similar for cations and anions, and give a quantitative measure of the sluggish dynamics of ions at relatively low temperature. To the best of our knowledge, no experimental data have been reported for this quantity, whose measurements might be beyond the reach of present techniques.

[5] The different dimensionality of the motion along z and in the xy plane has been taken into account by selecting the dimensionality d that appears in the Einstein relation for the diffusion constant (see, for instance [23]).

4. Summary and concluding remarks

Experimental results for thin IL films deposited on silica surfaces have been compared to simulation data for an idealized but still realistic atomistic model of the same interface.

AFM, in particular, has been used to image the topography and to estimate mechanical properties of thin [bmim][Tf_2N] films deposited by drop-casting on ordered and amorphous hydroxylated silica surfaces at ambient conditions. The collected images show a population of layered IL islands uniformly distributed on the solid surface. The islands' height reaches up to, and sometimes exceeds, ∼50 nm, while their lateral size extends up to a few μm. On amorphous silica, islands sometimes coexist with nanometric IL droplets, lying on top of the islands themselves, or directly in contact with the original silica surface.

The vertical organization of the islands consists of a regular succession of wide terraces delimited by sharp steps. Statistical analysis of the steps' height shows that layering has an underlying periodicity of $\delta = 0.56$ nm, virtually independent of the island shape and thickness. The geometric structure of the islands turns out to be surprisingly stable for a material whose bulk equilibrium phase is liquid at the temperature of our experiments, and AFM images are fully reproducible over times of several months, even when kept unprotected in contact with atmospheric air. The determination of mechanical properties confirms that the basic framework of islands is solid-like and remarkably rigid, even displaying a fragile fracture pattern.

Of course, the only conceivable reason for solid-like behaviour for the overlayer at a temperature at which ILs are, as their name implies, liquid ($T_m = 267$ K) is the interaction with the underlying solid substrate. Nevertheless, this observation is still particularly remarkable, given the fact that the height of the layered islands seen in our AFM images extends up to nearly 100 molecular layers, i.e. well into the mesoscopic range.

Simulations for a homogeneous [bmim][Tf_2N] film 4 nm wide in contact with a Si terminated, fully hydroxylated (111) β-cristobalite surface provide a microscopic view complementing the topographic images obtained by AFM. Samples have been equilibrated by annealing from high temperature (starting at $T = 600$ K), and production runs 5 ns long have been carried out at $T = 300$, 350 and 400 K. At these three temperatures, we observe large amplitude density oscillations arising from the IL interaction with the silica surface. At $T = 350$ and 400 K layering is confined to the very first molecular planes, while the rest of the film appears to be liquid-like. At $T = 300$ K, however, layering extends much deeper into the IL side of the interface, up to ∼2.5 nm. The identification of the thermodynamic state of the IL film at this temperature ($T = 300$ K) is somewhat uncertain. On the one hand, the IL overlayer is apparently disordered, and

displays some residual mobility of the ions. On the other hand, diffusion and relaxation are very slow on the simulation timescale, and several of the IL properties point to a glassy state. The periodicity ($\delta = 0.60$ nm) of the density oscillations depends only weakly on temperature, and closely matches the interlayer separation measured by experiments.

The role of surface hydroxylation in establishing layering has been investigated by repeating the $T = 300$ K simulation for a fully de-hydroxylated, neutral silica surface, obtained by replacing each of the original OH groups by a single O atom of reduced charge. This change affects the position and shape of the first IL layer in contact with the surface, but the effect is quantitatively small. On the other hand, removing the surface altogether restores the symmetry of the slab, and restores its fluid-like character. These observations are very important, since they confirm that the melting temperature of the IL model (not quantitatively determined in our study) is below $T = 300$ K, and every glassy or solid-like feature in the system structure and dynamics is due to the presence of the solid surface, apparently felt far away from the solid surface. Moreover, excluded volume effects, familiar from computational and simulation studies of simple liquids in contact with solid surfaces [22], are more important than specific adsorption, whose effect is fairly local.

While the similarities between the experimental and simulation results are encouraging, their differences might turn out to be more interesting. First of all, it is apparent that the general properties of layered islands are far more solid-like than in the simulation results. The difference might be due to a limitation of simulation, unable to nucleate a crystal-like phase for the overlayer during the nanosecond scale of our computations. On the other hand, unaccounted for details of experiments might also be responsible for the discrepancy. Drop-casting is a rather complex process, and, in principle, the results might depend on the deposition protocol. More importantly, impurities present on the surface might act like gelation agents able to change the state of the deposited film[6]. The most abundant contaminant present at oxide surfaces exposed to air is likely to be water. In most cases, water is expected to enhance fluidity and diffusion of ILs [27], but, in principle and only in special cases, it might act as a gelating agent by forming an extended network of hydrogen bonds. In this respect, it is important to consider that the IL used in our experiments and simulations is relatively hydrophobic, but it is also known to be weakly hygroscopic when exposed to air [28]. Computer simulations [29] show that, as expected, water in bulk [bmim][Tf_2N] tends to reside in proximity to the hydrophilic side of [Tf_2N]$^-$. In principle, one might speculate that, at precise stoichiometric composition, water and IL give rise to ordered structures whose melting temperature is higher than that of the pure and homogeneous IL. The formation of a solid-like overlayer, in any case, has to be a surface effect, since ordered water–[bmim][Tf_2N] has never been observed in the bulk, even when the IL is equilibrated in a wet atmosphere [28].

On the other hand, x-ray spectroscopy seems to exclude sizeable changes in the chemical composition of the film due to the methanol solvent used in the deposition, or due to decomposition of the IL [16].

In discussing the detailed comparison of experiments and simulations, however, it is essential also to consider that the silica surface described by our simulations is globally neutral, while real silica surfaces are known to acquire a small but non-negligible charge [10].

At present we are unable to unambiguously attribute the apparent difference in the overlayer self-organization to one or the other among the reasons proposed above. Further experimental and computational investigations, already partly under way, are needed to clarify this issue. The results might have a sizeable impact on applications such as lubrication, and perhaps electrochemistry and heterogeneous catalysis. On the other hand, they might point to important limitations of the computational model or of the simulation method, thus offering a useful opportunity to improve them.

Once the validity of the computational picture is clearly assessed, and possibly brought into agreement with the experimental one, simulation can be exploited to provide a wealth of microscopic information, partly inaccessible to experiments.

For instance, the analysis of simulation snapshots shows that the first IL layer in contact with silica, giving rise to a high and sharp density peak, is due primarily to the specific adsorption of the anion, hydrogen bonded to the OH groups at the solid surface. Local charge neutrality is restored by the adsorption of a nearly equivalent number of cations into this first layer, that appears depleted of butyl [bmim]$^+$ tails. The in-plane distribution of ions in this first plane contains remarkable seeds of crystal-like ordering, probably due to the regular corrugation of the underlying solid surface.

Charge neutrality is rather effectively enforced throughout the system, as shown by the detailed analysis of the charge density profile, and of the electrostatic signature of the interface. The positional ordering of ions apparent in the wide amplitude density oscillation at the interface is complemented by considerable orientational ordering, especially for the cations. Coupled to the uneven distribution of charge on the molecular ions, this ordering might give rise to a variety of paraelectric and ferroelectric configurations. Our simulation results might already contain hints of an incipient paraelectric to ferroelectric transition taking place at interfaces before the liquid to solid transition.

An additional interesting effect shown by simulations is the formation of a dense layer at the free IL surface. This is due to the tendency of the butyl tails to orient outwards, enhancing their orientational and rotational isomerization entropy. The depletion of hydrocarbon tails in the immediate sub-layer allows the tight packing of ions, that further decrease potential energy of the free surface.

The results obtained until now suggest several directions for further investigations. First of all, it is important to extend the close comparison of simulation and experiments to other interfaces, including both different ILs and different solid substrates. This might provide a very useful playground to validate, develop and improve computational models. In this respect, we point out that, while models for ILs in contact

[6] The formation of so-called ionogels obtained by mixing ILs with relatively small third species has been reported in [26].

with oxide surfaces might represent a fairly simple extension of present force field models already used for ILs, the modelling of interfaces with metals or semi-metals such as graphite is virtually unexplored or severely untested.

Acknowledgment

This project has been financially supported by Fondazione Cariplo under the grant 'Materiali e tecnologie abilitanti 2007'.

References

[1] Welton T 1999 *Chem. Rev.* **99** 2071
Holbrey J and Seddon K R 1999 *Clean Prod. Process.* **1** 223
[2] Liu X, Zhou F, Liang Y and Liu W 2006 *Wear* **261** 1174
Mu Z, Zhou F, Zhang S, Liang Y and Weimin L 2005 *Tribol. Int.* **38** 725
Liu W, Ye C, Gong Q, Wang H and Wang P 2002 *Tribol. Lett.* **13** 81
[3] See for instance the review in Aliaga C, Santos C S and Baldelli S 2007 *Phys. Chem. Chem. Phys.* **9** 3683
[4] Bovio S, Podestà A, Lenardi C and Milani P 2009 *J. Phys. Chem.* B **113** 6600
[5] Bovio S, Podestà A and Milani P 2009 *Ionic Liquids: From Knowledge to Application* (*ACS Symposium Series*) ed R D Rogers, N V Plechkova and K R Seddon (Washington, DC: American Chemical Society) at press
[6] Lynden-Bell R M and Del Pópolo M G 2006 *Phys. Chem. Chem. Phys.* **8** 949
Yan T, Li S, Jiang W, Gao W, Xiang W and Voth G A 2006 *J. Phys. Chem.* B **110** 1800
Bhargava B L and Balasubramanian S 2006 *J. Am. Chem. Soc.* **128** 10073
[7] Sloutskin E, Ocko B M, Tamam L, Kuzmenko I, Gog T and Deutsch M 2005 *J. Am. Chem. Soc.* **127** 7796
Bowers J and Vergara-Gutierrez B M 2004 *Langmuir* **20** 309
[8] Romero C, Moore H J, Lee T R and Baldelli S 2007 *J. Chem. Phys.* C **111** 240
Rivera-Rubero S and Baldelli S 2006 *J. Phys. Chem.* B **110** 15499
Rivera-Rubero S and Baldelli S 2006 *J. Phys. Chem.* B **110** 4756
[9] Carmichael A J, Hardacre C, Holbrey J D, Nieuwenhuyzen M and Seddon K R 2001 *Mol. Phys.* **99** 795
[10] Rollins J B, Fitchett B D and Conboy J C 2007 *J. Phys. Chem.* B **111** 4990
Fitchett B D and Conboy J C 2004 *J. Phys. Chem.* B **108** 20255
[11] Romero C and Baldelli S 2006 *J. Phys. Chem.* B **110** 6213
[12] Mezger M *et al* 2008 *Science* **322** 424
[13] Seifert N and Wipff G 2008 *J. Chem. Phys.* C **112** 19590
[14] Liu L, Li S, Cao Z, Peng Y, Li G, Yan T and Gao X-P 2007 *J. Phys. Chem.* C **111** 12161
[15] Maolin S *et al* 2008 *J. Chem. Phys.* **128** 134504
[16] Butt H-J, Cappella B and Kappl M 2005 *Surf. Sci. Rep.* **59** 1
[17] Canongia Lopes J N and Pádua A A H 2004 *J. Phys. Chem.* B **108** 16893
[18] Giovambattista N, Rossky P J and Debenedetti P G 2006 *Phys. Rev.* E **73** 041604
Giovambattista N, Debenedetti P G and Rossky P J 2007 *J. Phys. Chem.* B **111** 9581
[19] Smith W, Leslie M and Forester T R 2003 *DL-POLY, Version 2.14* Daresbury Laboratories, Daresbury, Warrington, UK
[20] Zhuravlev L T 1987 *Langmuir* **3** 316
[21] Halka V, Tsekov R and Freyland W 2005 *J. Phys.: Condens. Matter* **17** S3325
[22] Snook I K and Henderson D 1984 *J. Chem. Phys.* **68** 2134
[23] Hansen J P and MacDonald I R 1976 *Theory of Simple Liquids* (London: Academic)
[24] Dzyuba S V and Bartsch R A 2002 *Chem. Phys. Chem.* **3** 161
[25] Arce A, Rodrigues O and Soto A 2004 *J. Chem. Eng. Data* **49** 514
[26] Kimizuka N and Nakashima T 2001 *Langmuir* **17** 6759
Kubo W, Kitamura T, Hanabusa K, Wada Y and Yanagida S 2002 *Chem. Commun.* 374–5
[27] Menjoge A, Dixon J N, Brennecke J F, Maginn E J and Vasenkov S 2009 *J. Phys. Chem.* B **113** 6353
[28] Jacquemin J, Husson P, Padua A A H and Majer V 2006 *Green Chem.* **8** 172
Huddleston J G, Visser A E, Reichert W M, Willauer H D, Broker G A and Rogers R D 2001 *Green Chem.* **3** 156
Seddon K R, Stark A and Torres M-J 2000 *Pure Appl. Chem.* **72** 2275
[29] Sieffert N and Wipff G 2006 *J. Phys. Chem.* B **110** 13076